Spectral and thermodynamic properties of a Fibonacci quasicrystal

1992 J. Phys. A: Math. Gen. 25 577

(http://iopscience.iop.org/0305-4470/25/3/016)

J. Phys. A: Math. Gen. 25 (1992) 577-588. Printed in the UK

Spectral and thermodynamic properties of a Fibonacci quasicrystal

R K Pattnaik and Edward A Whittaker

Department of Physics and Engineering Physics, Stevens Institute of Technology, Hoboken, NJ 07030, USA

Received 30 December 1990

Abstract. We present calculations leading to the phonon density of states in a Fibonacci quasicrystal with fixed end-points. The method is based on a selective elimination process and the results show that the system at low frequencies has the behaviour of a periodic lattice. The high-frequency end of the spectrum is found to have large forbidden bands and in the limit of longer chains the higher-frequency modes are seen to be suppressed. The density of state function has further been used to calculate the heat capacity which is found to be lower than its periodic counterpart. The electronic energy has been calculated from the associated transmission coefficient and the results show that the spectrum is largely band-like, in contrast to the uniform scaling structure which has been reported. It is also shown that in the limit the quasicrystal reduces to a periodic structure; the calculations reproduce the usual results.

1. Introduction

The discovery [1, 2] of a phase of AlMn exhibiting icosahedral symmetry (termed 'quasicrystal') in its diffraction pattern has drawn considerable attention from both experimental and theoretical sectors. Substantial progress has been made in understanding this material in terms of a quasiperiodic lattice. In an attempt to explain its diffraction pattern two major approaches for geometrical construction of a quasilattice have emerged. One method, due to Levine and coworkers [3], follows the idea of generating the quasilattice from a Penrose tiling which consists of two unit cells (rhombuses in 2D and rhombohedra in 3D). The two unit cells are repetitively used following certain matching rules to form the quasilattice. The other approach developed by Zia and others [4] is based on the idea that a quasilattice can be seen as a hypersurface in a higher-dimensional periodic lattice. Apart from these two approaches other models are also available in the literature [5].

In addition to its geometric structure, attention has also been focused on understanding the physical properties of the quasicrystal. Because of mathematical complexities most of the work has been restricted to one-dimensional quasicrystals. The standard one-dimensional system that has been the subject of extensive study is the Fibonacci lattice. This lattice can be generated from two basis vectors of length a and b by successive application of the rule

$$S_{n+1} = S_{n-1}S_n \tag{1}$$

where $S_0 = a$ and $S_1 = b$ and a is equal to τb, τ being the golden mean $(\sqrt{5}+1)/2$. The study of electronic energy spectra was initiated by Khomoto and Banavar [6] (based on a previous work [7]) and pursued by several other groups [8, 9]. In their work,

0305-4470/92/030577+12$04.50

which uses the renormalization approach, a Schrödinger equation is written in terms of dynamic transfer matrices. It was then shown that the trace of these matrices can define a simple dynamic mapping. Allowed and forbidden energy eigenvalues were found from a fixed-point analysis of the mapping. Numerical results presented show that the energy spectrum is self-similar and the eigenstates can have critical structure.

The phonon problem has also been addressed on the lines of the renormalization group method [6], leading to the conclusion that the phonon spectra is self-similar. A more direct and transparent approach, not following the renormalization group approach, was taken by Lu and coworkers [10] to study the vibration spectrum of a Fibonacci quasicrystal with fixed end-points. More recently, Ashroff and Stoinchcombe [11] have used the Green function approach to investigate the density of states and eigenvalues for both electron and phonon spectra of a Fibonacci quasicrystal. In an excellent work Chakrabarti *et al* [12] have followed the same formalism to study the local density of states of an infinitely long Fibonacci chain.

The Fibonacci quasicrystal has been grown in the laboratory. Merlin and coworkers [13] have been able to grow layers of GaAs–AlAs in a Fibonacci sequence and have made x-ray and Raman scattering measurements.

In the present work we address the phonon, thermodynamic and electronic properties of a finite Fibonacci quasicrystal. The major difference between our work and most others published is that we do not use a dynamic mapping to study the system. In section 2 we discuss the vibration problem of a Fibonacci quasicrystal with fixed end-points on the basis of selective elimination. This method is based on the work of Goncalves de Silva and Koiller [14] for the study of local density of states of disordered chains and studied in more detail by Southern and others [15]. In order to understand the selective elimination we note that a Fibonacci sequence at any generation can reduce to its preceding sequence with different bonds by introducing a scale transformation. This transformation amounts to eliminating the displacement of those lattice sites that are connected to the left by an a bond and to the right by a b bond and thereby reducing the number of equations. In the process of this elimination we will show that the coefficients of the equations take on a very simple recursive form and also the structure of the equations stays unchanged. Hence, it is possible to calculate the coefficients after any number of selective eliminations. This enables us to reduce $F(n)$ bonds and hence $F(n)$ equations to one equation by a finite number of iterations. Here the Fibonacci number $F(n)$ is defined through the relation $F(n+1)=F(n)+F(n-1)$ where $F(0)=1$ and $F(1)=1$. The resulting equation can be solved numerically. We use this technique to study the vibration problem in the next section.

In section 3 we study the electron band structure. We note that in a solid an electron in an allowed band has an extended state function in contrast to the localized core states. If the solid is modelled following Kronig–Penney as an array of potential barriers, then an electron in an extended energy state can tunnel across all the barriers. In other words it will have a large coefficient of transmission for barrier penetration. On the other hand, if it falls in a forbidden band it cannot tunnel and its transmission coefficient will fall to zero after a few barriers. Using the above arguments we first calculate the electron energy spectra of a periodic system exactly reproducing the results of Kronig–Penney and then we apply the same technique to a chain of potential barriers whose separations follow a Fibonacci sequence. The results will be shown to be in good agreement with the dynamical mapping approach.

It may be noted that in all our calculations when the length of both the basis vectors a and b in the quasicrystal are made equal we recover the usual periodic lattice results.

2. Phonon spectrum

Let us consider a one-dimensional chain of atoms separated from each other by lattice constants a or b with the associated spring constants being k_a and k_b. As pointed out in the introduction, the lattice constants a and b define a Fibonacci sequence through relation (1).

The equation of motion of the nth atom of the chain is given by

$$m\frac{\partial^2 u_n(x,t)}{\partial t^2} = k_{n,n+1}(u_{n+1}-u_n)+k_{n-1,n}(u_{n-1}-u_n) \tag{2}$$

where m is the mass of the atom, $u_n(x,t)$ is the displacement of the nth atom from equilibrium and k_{n+j} is the spring constant between the nth and $(n+j)$th atoms. Here we consider only nearest-neighbour interactions, i.e. $j=\pm 1$. Assuming harmonic time dependence we obtain

$$(k_{n,n+1}+k_{n-1,n}-m\omega^2)u_n = k_{n,n+1}u_{n+1}+k_{n-1,n}u_{n-1}. \tag{3}$$

If $a=b$, then $k_a=k_b$ and $u_n(x)$ are just the Bloch functions for phonons. However, for the present case the Bloch theorem is not applicable and, therefore, we cannot assume wave-like displacements.

In order to solve equation (3) we impose the boundary condition that the end-points of the chain are fixed (i.e. $u_0=0=u_N$). A similar system has been studied by Lu *et al* [10] using the transfer matrix method. Here, we follow the decimation approach of Goncalves da Silva and Koiller [14]. Consider a chain of nine atoms having eight bonds in a Fibonacci sequence. We note that each atom is connected to the left and right by a pair of spring constants that are either k_a and k_b, k_b and k_a, or k_a and k_a. These three possibilities are invariant under the elimination process and in order to exploit this fact we introduce the following constants:

$$\begin{aligned} k_a(0) &= k_a \\ k_b(0) &= k_b \\ k_1(0) &= k_b(0)+k_a(0) \\ k_2(0) &= k_a(0)+k_b(0) \\ k_3(0) &= k_a(0)+k_a(0). \end{aligned} \tag{4}$$

In terms of the above constants the equation of motion (equation (3)) for each atom of the chain may be written

$$n=1 \qquad (k_1(0)-m\omega^2)u_1 = k_b(0)u_2+k_a(0)u_0 \tag{5}$$

and likewise for the other eight sites.

Now let us introduce the transformation

$$a(0)+b(0)=a(1) \qquad a(0)=b(1) \tag{6}$$

where $a(0)=a$ and $b(0)=b$. Under the above transformation the chain which had eight bonds originally reduces to five bonds, which amounts to eliminating the displacement of those atoms that are connected to the left by an a bond and to the right by a b bond. In other words we need to eliminate u_1, u_4 and u_6 from equations (5), obtaining

$$\left(k_2(0)-\frac{k_b^2(0)}{k_1(0)-m\omega^2}-m\omega^2\right)u_2 = k_a(0)u_3+\frac{k_a(0)k_b(0)}{k_1(0)-m\omega^2}u_0 \tag{7}$$

and similar equations for u_3, u_5 and u_7. In the decimated chain each atom is connected by a pair of spring constants, although of different strength, that again falls into one of the three possibilities. This invariance enables one to renormalize the constants defined in equation (7) and by inspection they can immediately be identified as

$$\begin{aligned}
k_a(n) &= \frac{k_a(n-1)k_b(n-1)}{k_1(n-1)-m\omega^2} \\
k_b(n) &= k_a(n-1) \\
k_1(n) &= k_2(n-1)-\frac{k_b^2(n-1)}{k_1(n-1)-m\omega^2} \\
k_2(n) &= k_3(n-1)-\frac{k_a^2(n-1)}{k_1(n-1)-m\omega^2} \\
k_3(n) &= k_2(n-1)-\frac{k_a^2(n-1)+k_b^2(n-1)}{k_1(n-1)-m\omega^2}
\end{aligned} \tag{8}$$

where n is the number of decimation transformations made on the chain.

The above form shows recursive structure of the constants at each stage of decimation. Further elimination of u_2 and u_7 from equations (7) reduces the number of equations to two with the ks defined through equations (8) with $n=2$ as expected. This recursive structure is a consequence of the invariance of the three possible spring constant pairs an atom can have at any stage of decimation. Furthermore, this invariance is expected because the Fibonacci sequence reduces to its preceding one (except for a scalar factor) under each decimation.

With the boundary conditions, i.e. $u_0=0=u_N$, the last two equations can easily be solved for the eigenfrequencies. The elegance of the method lies in this ability to reduce the original 7×7 matrix of equation (5) into a 2×2 matrix by two stages of selective elimination. In this manner the equation of motion for a chain of atoms with fixed end-points, at any generation of the Fibonacci sequence, can be reduced to solving the determinant

$$\begin{vmatrix} k_1(n)-m\omega^2 & -k_b(n) \\ -k_b(n) & k_2(n)-m\omega^2 \end{vmatrix} = 0 \tag{9}$$

for the squared eigenfrequencies of the system where n is the number of decimations and $k_1(n)$, etc, are related to the preceding stage through equations (8). Once the roots of the determinant in equation (9) are known, the density of states for the squared eigenfrequencies can be found using the relation [16, p 40]

$$D(\omega^2)=\frac{1}{\pi}\operatorname{Im}\left[\lim_{\varepsilon\to0}\lim_{N\to\infty}\left(\frac{1}{N}\sum_{\text{all roots}}\frac{1}{\omega_j^2-\omega^2-\mathrm{i}\varepsilon}\right)\right] \tag{10}$$

where ω_j^2 are the roots of equation (9) and the role of the small imaginary part $\mathrm{i}\varepsilon$ is to ensure convergence. However, since the roots of the determinant in equation (9) are quasi-continuously distributed, we can break the frequency space into arbitrarily narrow strips and in each strip the roots, ω_j^2, will differ from each other infinitesimally. As a result we can approximate the summation over the roots in the last equation by a summation over the number of roots in each strip. Quantitatively, if ω_j^2 is the centre frequency of the jth strip of width $\mathrm{d}\omega^2$ and $n(\omega_j^2)$ is the number of roots of the

determinant in equation (9) between ω_j^2 and $(\omega_j^2 \pm d\omega^2)/2$, then the last equation takes the form

$$D(\omega^2) = \frac{1}{\pi} \operatorname{Im}\left[\lim_{\varepsilon \to 0} \lim_{N \to \infty} \left(\frac{1}{N} \sum_{\text{all strips}} \frac{n(\omega_j^2)}{\omega_j^2 - \omega^2 - i\varepsilon}\right)\right]. \tag{11}$$

We have used this expression to calculate the $D(\omega^2)$ which can be related to the density of states $g(\omega)$ through the relation [17]

$$g(\omega) = 2\omega D(\omega^2). \tag{12}$$

In the following two cases we discuss the results of our calculations first applied to a periodic case and then to a Fibonacci chain. Finally, we also discuss heat capacities of both the systems.

2.1. Periodic chain

In order to test our formalism we first set the spring constants equal, i.e. $k_a = k_b = k$, thereby having a chain of atoms periodically spaced. In this limit the squared frequency density of states, as given by Hori [16, p 31] is

$$D(\omega^2) = \frac{2}{\pi\omega\sqrt{\omega_m^2 - \omega^2}} \tag{13}$$

where $\omega_m^2 = 4k/m$, showing singularities at $\omega = 0$ and at $\omega = \omega_m$. The same quantity calculated with our formalism is shown in figure 1(a), confirming the analytical result,

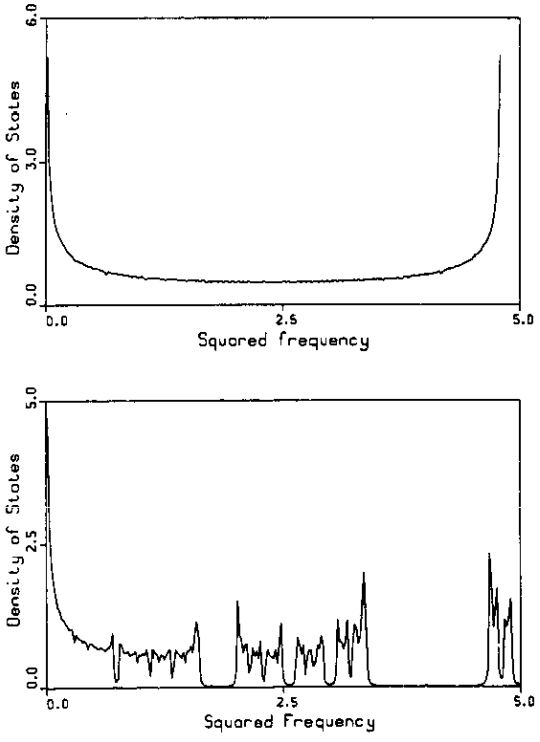

Figure 1. Plot of phonon density of states for a (a) periodic and a (b) Fibonacci lattice. There are 4182 sites with $k_a = 1.2$ N m^{-1} and $k_b = \tau k_a$, where $\tau = (\sqrt{5}+1)/2$ and the density of states is in hertz^{-2}. In part (a) $k_b = k_a = 1.2$ N m^{-1}.

equation (17). In our case we have taken $k = 1.2$ (with $\varepsilon = 0.005$ and $N = 4181$) and we have observed from our calculation that when $m\omega^2 > 4.8$, the determinant (13) does not have any roots, which is indeed expected.

2.2. Fibonacci chain

When $k_a \neq k_b$ we have a Fibonacci quasicrystal and the spectrum as shown in figure 1(b), for the same N, and ε is quite different from that of the periodic case except in the low-frequency range. The spectrum has forbidden bands of frequencies of various widths, with a wide gap at high frequency. The allowed frequency structure, particularly in the high-frequency zone, approaches a set of isolated delta function singularities, which are broadened due to our numerical method. If the narrow gaps are ignored, the spectrum is band-like and is seen to have Van Hove-type singularities at the band edges.

The spectrum is self-similar in structure. When the central part of figure 1(b) is expanded as shown in figure 2(a) it has the same structure as the original one. The allowed zones are thus seen to occupy a fairly small portion of the total band.

As the number of atoms in the chain are increased there is a decrease in the phonon density of states and the high-frequency modes are further suppressed. The results are shown in figure 2(b) for $N = 46\,368$ bonds. This would indicate that, in the limit of an infinitely long chain, only low-frequency modes would propagate and high-frequency

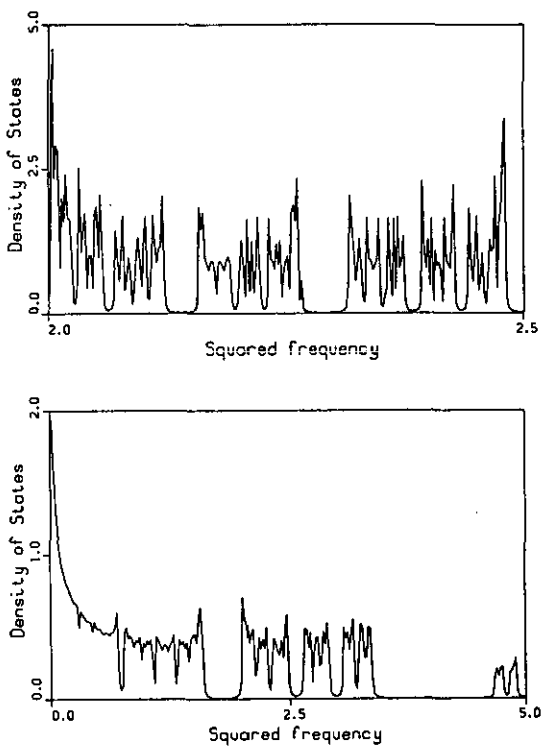

Figure 2. (a) Enlarged view of the middle band of figure 1(b) showing self-similarity in its structure. (b) Same as the plot of figure 1(b) except that the lattice has 46 368 sites; a decrease in the phonon density of states and wider band gap in the higher-frequency end is shown.

modes would be heavily damped. We interpret this damping as follows. In a periodic system undergoing vibration the phase difference between any two consecutive lattice sites is a constant (which follows from the Bloch theorem). This constancy enables the system to sustain a normal mode and hence a well-defined dispersion relation. But for a Fibonacci lattice such a relation does not exist. In other words the phase difference between any two consecutive lattice sites is uncorrelated. At low frequencies, however, this lack of correlation is very weak and the system responds in a similar way to the periodic lattice. This can be seen at the lower-frequency end in figure 1(*b*). But as the frequency is increased the lack of correlation becomes large enough to suppress the high-frequency modes in a very short time. This suppression becomes more pronounced as the chain length increases.

3. Thermodynamic properties

We now calculate the Debye model heat capacity of the Fibonacci quasicrystal using [18]

$$C_V = \frac{\partial U}{\partial T}$$

where

$$U = \int \mathrm{d}\omega\, g(\omega) n(\omega, T) \hbar\omega$$

with U and $n(\omega, T)$ being, respectively, the total thermal energy and the Planck distribution function, and T the temperature. For compatibility with our numerical data, we replace the integration for the thermal energy by the summation

$$U = \sum_i \frac{n(\omega_i)\hbar\omega_i}{\mathrm{e}^{\beta\hbar\omega_i} - 1} \tag{14}$$

where $\beta = 1/k_B T$, k_B being the Boltzmann constant. In figure 3 we have plotted the heat capacities for both the periodic and Fibonacci chains. The latter has a smaller

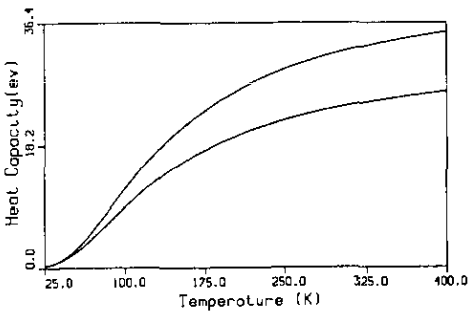

Figure 3. Plot of the heat capacity for a periodic and Fibonacci lattice. The periodic system (the upper plot) shows a higher heat capacity than the Fibonacci lattice. The temperature is in kelvins and the heat capacity is in electron volts per kelvin.

heat capacity compared with the periodic one. At low temperatures they both have almost the same heat capacity but, as the temperature increases, they split, the crystal showing larger capacity. Figures 1(a) and 1(b) show that within a given range of frequencies the Fibonacci lattice has a smaller total number of phonon states than the regular crystal, accounting for the smaller heat capacity.

4. The electronic energy spectrum

In this section we consider the electronic energy spectrum of a Fibonacci lattice. Our crystal is derived from the Kronig–Penney model but with two lattice constants a and b arranged according to the Fibonacci sequence.

If the system is periodic, one can solve the Schrödinger equation in conjunction with the Bloch theorem, which leads to Bloch-type wavefunctions with energy bands. Since the Fibonacci lattice does not satisfy the Bloch theorem, we follow a different approach. The method is based on computing the transmission coefficient for an electron to penetrate through all barriers of the system. The transmissibility is then used to determine the allowed and forbidden energy bands. It can further be shown that this formalism—without use of the Bloch theorem—leads exactly to the results of the Kronig–Penney model for the periodic case when the transmission coefficient is made unity.

Let us consider potential barriers of height V and width d forming a Kronig–Penny model Fibonacci crystal with lattice parameters a and b.

Assuming the potential to be zero in the jth region, the solution to the Schrödinger equation is

$$\Psi_j(x) = (A_j\, e^{-ikx_j})\, e^{ikx} + (B_j\, e^{ikx_j})\, e^{-ikx}. \tag{15}$$

and, in the $(j+1)$th region, the potential being V, yields the solution

$$\Psi_{j+1}(x) = (A_{j+1}\, e^{-Kx_{j+1}})\, e^{Kx} + (B_{j+1}\, e^{Kx_{j+1}})\, e^{-Kx}. \tag{16}$$

where $k^2 = 2mE/\hbar^2$ and $K^2 = 2m|E - V|/\hbar^2$.

Matching the boundary conditions at $x = x_j$ it can be shown that

$$\begin{pmatrix} e^{ik\Delta x_j} & e^{-ik\Delta x_j} \\ \alpha\, e^{ik\Delta x_j} & -\alpha\, e^{-ik\Delta x_j} \end{pmatrix} \begin{pmatrix} A_j \\ B_j \end{pmatrix} = \begin{pmatrix} 1 & 1 \\ 1 & -1 \end{pmatrix} \begin{pmatrix} A_{j+1} \\ B_{j+1} \end{pmatrix} \tag{17}$$

where $\alpha = ik/K$ and Δx_j is the width of the region between the jth and $(j+1)$th potential barrier, which can be a or b.

Similarly, by considering the $(j+1)$th and $(j+2)$th regions an identical relation can be established where $ik\Delta x$ and α would be replaced by Kd and α^{-1}.

Eliminating A_{j+1}, we get an equation involving all the parameters of the system, which establishes a relation between the jth and $(j+2)$th valleys having the $(j+1)$th barrier in between them. Iterative use of it enables us to connect the incident and transmitted wavefunctions through the equation

$$\begin{pmatrix} A_1 \\ B_1 \end{pmatrix} = \prod_{j=1}^{N} (\bar{u}(ik\Delta x_j, Kd)) \begin{pmatrix} A_{2N+1} \\ 0 \end{pmatrix} \tag{18}$$

where $\bar{u}$ is the matrix obtained in eliminating A_{j+1}, N is the number of barriers and

A_{2N+1} is the amplitude of the wavefunction of the electron after it has tunnelled through all the N barriers.

Using the Kronig-Penney limit

$$\lim_{V\to\infty}\lim_{d\to 0} Vd = \text{constant} \tag{19}$$

and the matrices of equation (17), the product in equation (18) may be evaluated and cast in the form

$$\prod_{j=1}^{N} \bar{u} = \prod_{j=1}^{N} \begin{bmatrix} (1-P/\mathrm{i}kb)\,\mathrm{e}^{-\mathrm{i}k\Delta x_j} & -P/\mathrm{i}kb\,\mathrm{e}^{-\mathrm{i}k\Delta x_j} \\ P/\mathrm{i}kb\,\mathrm{e}^{\mathrm{i}k\Delta x_j} & (1+P/\mathrm{i}kb)\,\mathrm{e}^{\mathrm{i}k\Delta x_j} \end{bmatrix} \tag{20}$$

where $P = mVbd/\hbar^2$. If the elements of the matrix after multiplying out all the N matrices on the right-hand side of the above equation are denoted by g_{ij} then, from equation (18), the associated coefficient of transmission is given by

$$T = \left|\frac{A_{2N+1}}{A_1}\right|^2 = \left|\frac{1}{g_{11}(a, b, P, N, \mathrm{i}k)}\right|^2. \tag{21}$$

T is then computed as a function of the electron energy and an allowed band is identified as those energy values which make $T>0$. For $T>0$ the electron has a continuous probability distribution function across the whole length of the crystal, reflecting the behaviour of an extended wavefunction associated with the electrons in the allowed bands of a solid. Since the above formalism is based on a numerical evaluation of T using equation (21), it fails to correctly predict the band edges. However, the calculations show that, as E approaches a forbidden band, T very sharply falls to as low as 0.001 and rises equally fast to as high as 0.99 on the other end of the forbidden band. Transmission coefficients computed for various periodic and Fibonacci systems show bands of transmission and non-transmission with well-defined edges. Further calculation shows that as the number of barriers are increased the band edges become sharper.

In the following subsections we apply the above formalism to the periodic crystal and the Fibonacci quasicrystal.

4.1. Periodic lattice

If $a = b$ the system reduces to a periodic crystal and, in that limit, we should reproduce the results of the Kronig-Penney model. In order to show that we first calculated g_{ij} as function of the incident wavenumber k, which in turn is used to calculate T as a function of k. The allowed band structure is obtained from the equation $E = \hbar^2k^2/2m$.

Figure 4(a) shows a plot of E versus k. We have taken $N = 4181$ and $P = 3\pi/2$. Although k is not a good quantum number associated with the crystal, it may be used to illustrate the qualitative structure of the bands. From the figure we observe that:

(i) The energy spectrum is band-like with bandwidths increasing as the energy increases.

(ii) Band gaps appear at $ka \simeq \pi, 2\pi, 3\pi$.

(iii) The width of the forbidden bands narrows down with increasing energy, characteristic of the Kronig-Penney model. In the limit $a = b$ the present formalism for $T = 1$ reduces to the exact analytical result of the Kronig-Penney model.

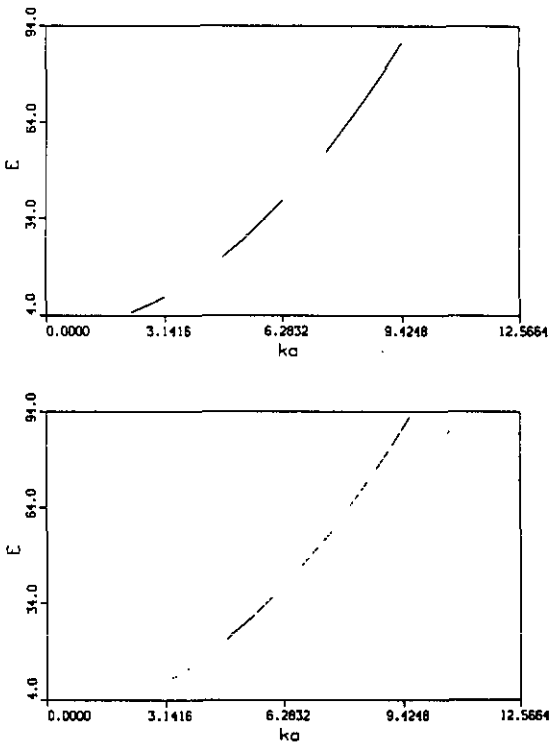

Figure 4. (*a*) Plot of the energy band structure for a periodic lattice having 4182 potential barriers. Band gaps with widths narrowing appear at π, 2π and 3π, and allowed bands widen as 'ka' increases. The energy is in units of $\hbar^2/2ma^2$ with $a = 1.0$ nm and $P = 3\pi/2$. (*b*) Same plot as in (*a*) but for a Fibonacci lattice. It has a band structure but with numerous sub-bands. Here $b = 1.0$ nm and $a = \tau b$ where $\tau = (\sqrt{5}+1)/2$. The states at the lower end of the spectrum indicate localization.

4.2. Fibonacci lattice

When a and b are not equal we have a Fibonacci quasicrystal. The energy spectrum is shown in figure 4(*b*) for 4181 cells with $P = 3\pi/2$. We observe from the plots that:

(i) Although the energy spectrum is band-like in a broad sense, each band consists of sub-bands having narrow gaps.

(ii) The energy band is self-similar. When any particular band is expanded it has a structure similar to the original one. In figure 5(*a*) we have expanded a small section of figure 4(*b*), and figure 5(*b*) shows a further expansion of a small section of figure 5(*a*). The structure is seen to reproduce itself and, in view of that, we may say that in the limit of an infinitely long crystal the spectrum would be Cantor-like. This fact has also been reported by Khomoto and Banavar [6] using renormalization theory.

(iii) Careful examination of figure 4(*b*) and a similar result for a chain of 89 barriers shows that as the number of barriers are increased the lower energy band narrows down. We interpret this to mean that in the limit of longer chains the lower-energy states are localized to smaller regions of the crystal, unlike the higher-energy states which are extended throughout the crystal.

According to the results of Khomoto and Banavar [6] the electronic energy spectrum has a uniform scaling. Our calculations, however, do not show this behaviour. This,

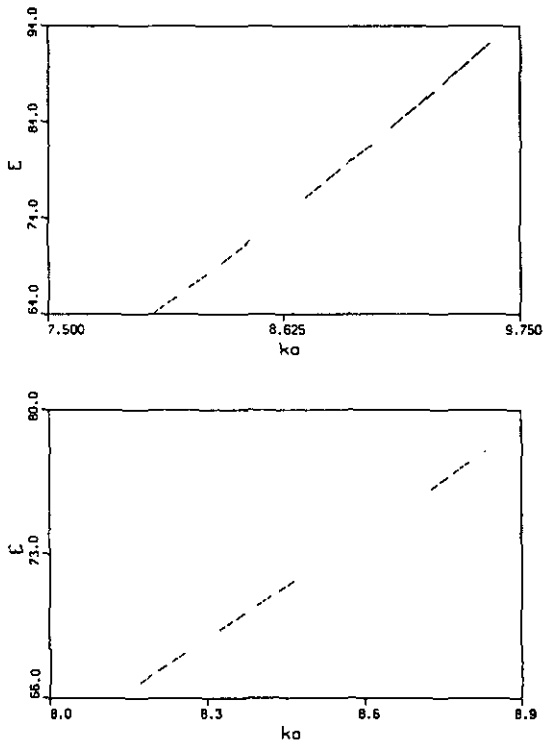

Figure 5. (*a*) Enlarged view of one of the bands of figure 4(*b*). (*b*) Further enlargement of a section of part (*a*). Both plots reveal self-similar structure of the spectrum.

we believe, is due to the tight binding model assumed in their discussion of the spectrum where the wavefunction is presumed to be atomic-like on the lattice site and negligibly small in the intersite space, which may not be a correct assumption. On the contrary, in our method we assume a continuous state function for the electrons across the whole length of the crystal in an allowed energy band.

5. Conclusion

We have addressed the phonon and electronic energy spectra of a one-dimensional Fibonacci lattice. We have used a selective elimination approach to find the density of states of the system without involving any approximations, in contrast to the local density of states as reported by Chakrabarti *et al* [12]. In the low-frequency regime the superlattice behaves similarly to that of a periodic system. However, as the frequency is increased, forbidden bands appear and their width increases as the frequency is increased. The density of state function shows Van Hove-like singularities at the band edges. The spectrum has a self-similar structure and the density of states has been found to decrease as the length of the chain is increased. This decrease is believed to be due to lack of correlation in the phase relationship between sites. This dependence of the density of states on the length of the chain has not been reported in the works of others [11, 12], which are based on renormalization of an infinitely long Fibonacci chain.

The density of states as calculated in the present formalism has the advantage that it enables one to study the thermodynamic properties of the system. The heat capacity of the system has been calculated and it is found to be lower than its periodic counterpart.

The electronic energy spectrum has been addressed by a novel method. We have calculated the electronic energy spectrum from the transmission coefficient without using any approximations other than that of Kronig-Penney. The results show that the energy spectrum is band-like with numerous gaps, and does not show the structure of uniform scaling as reported previously [6]. This difference, as we have mentioned earlier, is believed to be due to the tight binding models considered in the dynamical mapping approach. It too has a self-similar structure and indications of localization. When the present manuscript was under consideration by the publishers a similar work on tunnelling through Fibonacci barriers was reported by Kiang *et al* [19].

Acknowledgments

We gratefully acknowledge Dr G Gumbs for reviewing the manuscript critically and drawing our attention to certain mistakes in the calculations. We are very thankful to him for his suggestions to improve the results for the phonon density of states. We also gratefully acknowledge Dr H Cui for useful discussions.

References

[1] Shechtman D, Blech I, Gratias D and Cahn J W 1984 *Phys. Rev. Lett.* **53** 1951
[2] Jarić M V 1989 *Aperiodicity and Order* vols 1 and 2 (London: Academic)
Janot Ch and Dubois J M 1988 *Quasicrystalline Materials* (Singapore: World Scientific)
Steinhardt P J and Ostlund S 1987 *The Physics of Quasicrystals* (Singapore: World Scientific)
[3] Levine D and Steinhardt P J 1984 *Phys. Rev. Lett.* **53** 2477
[4] Zia R K and Dallas W J 1985 *J. Phys. A: Math. Gen.* **18** L341
Kalugin P A, Kitaev A Yu and Levitov L S 1985 *JETP Lett.* **41** 145
Elser V 1986 *Acta Cryst.* A **42** 36
[5] Bak P 1986 *Scr. Metall.* **20** 181
Socolar J E S and Steinhardt P J 1986 *Phys. Rev.* B **34** 617
[6] Kohmoto M and Banavar J R 1986 *Phys. Rev.* B **34** 563
[7] Gumbs G and Ali M K 1988 *Phys. Rev. Lett.* **60** 1081
Kohmoto M, Kadanoff L P and Tang C 1983 *Phys. Rev. Lett.* **50** 1870
Ostlund S, Pandit R, Rand D, Schellnhuber H J and Siggia E D 1983 *Phys. Rev. Lett.* **50** 1873
Luck J M and Nieuwenhuizen Th M 1986 *Europhys. Lett.* **2** 257
Fujita M and Machida K 1986 *Solid State Commun.* **59** 61
Luck J M and Petritis D 1986 *J. Stat. Phys.* **42** 289
[8] Kohmoto M and Sutherland B 1986 *Phys. Rev. Lett.* **56** 2740
[9] Odagaki T and Nguyen D 1986 *Phys. Rev.* B **33** 2184; 1986 *Phys. Rev.* B **34** 2740
[10] Lu J P, Odagaki T and Birman J L 1986 *Phys. Rev.* B **33** 3809
[11] Ashraff J A and Stoinchcombe R B 1988 *Phys. Rev.* B **37** 5723
[12] Chakrabarti A, Karmakar S N and Moitra R K 1989 *J. Phys.: Condens. Matter* **1** 1017
[13] Merlin R, Bajema K, Clarke R, Juang F T and Bhatacharya P K 1985 *Phys. Rev. Lett.* **55** 1768
[14] Goncalves da Silva C E T and Koiller B 1981 *Solid State Commun.* **40** 215
[15] Southern B W, Kumar A A and Ashraff J A 1983 *Phys. Rev.* B **28** 1785
Langlois J M, Trembley A M S and Southern B W 1983 *Phys. Rev.* B **28** 218
[16] Hori J 1973 *Spectral Properties of Disordered Chains and Lattices* (Oxford: Pergamon)
[17] Jones W and March N H 1973 *Theoretical Solid State Physics* (New York: Dover) p 238
[18] Kittel C 1985 *Introduction to Solid State Physics* 5th edn (New York: Wiley) pp 130-1
[19] Kiang D, Ochiai T and Datá S 1990 *Am. J. Phys.* **58** 1200